

RESEARCH ARTICLE



Targeted delivery of galunisertib using machine perfusion reduces fibrogenesis in an integrated *ex vivo* renal transplant and fibrogenesis model

L. Leonie van Leeuwen^{1,2,3} | Mitchel J. R. Ruigrok⁴ | Benedikt M. Kessler² |
Henri G. D. Leuvenink¹ | Peter Olinga⁴

¹Department of Surgery, University Medical Center Groningen, University of Groningen, Groningen, The Netherlands

²Nuffield Department of Medicine, Centre for Medicines Discovery, Target Discovery Institute, University of Oxford, Oxford, UK

³Recanati/Miller Transplantation Institute, Icahn School of Medicine at Mount Sinai, New York City, New York, USA

⁴Department of Pharmaceutical Technology and Biopharmacy, Groningen Research Institute of Pharmacy, University of Groningen, Groningen, The Netherlands

Correspondence

L. Leonie van Leeuwen, Department of Surgery, University Medical Center Groningen, University of Groningen, Hanzeplein 1, 9713 GZ Groningen, The Netherlands.
Email: l.l.van.leeuwen@umcg.nl

Abstract

Background and Purpose: Fibrosis in kidney allografts is a major post-transplant complication that contributes to graft failure. Lately, multiple potent inhibitors of fibrosis-related pathways have been developed such as galunisertib, an inhibitor of the transforming growth factor-beta (TGF- β /TGF β 1) signalling pathway. This drug, however, poses risks for adverse effects when administered systemically. Therefore, we devised a new repurposing strategy in which galunisertib is administered *ex vivo*. We combined machine perfusion and tissue slices to explore the antifibrotic effects of galunisertib in renal grafts.

Experimental Approach: Porcine kidneys were subjected to 30 min of warm ischaemia, 24 h of oxygenated hypothermic machine perfusion and 6 h of normothermic machine perfusion with various treatments (i.e. untreated control, TGF β 1, galunisertib or TGF β 1 + galunisertib; $n = 8$ kidneys per group). To determine whether effects persisted upon ceasing treatment, kidney slices were prepared from respective kidneys and incubated for 48 h.

Key Results: Galunisertib treatment improved general viability without negatively affecting renal function or elevating levels of injury markers or by-products of oxidative stress during perfusion. Galunisertib also reduced inflammation and, more importantly, reduced the onset of fibrosis after 48 h of incubation.

Conclusions and Implications: Our findings demonstrate the value of using machine perfusion for administering antifibrotic drugs such as galunisertib, proving it to be an effective example of repurposing.

KEYWORDS

fibrogenesis, interstitial fibrosis and tubular atrophy, ischaemia-reperfusion injury, normothermic machine perfusion, renal transplantation, repurposing

Abbreviations: Col1a2, collagen alpha-2(I) chain; HSP47/Serpinh1, heat shock protein 47/serpin family H member 1; PAI-1/Serpine1, plasminogen activator inhibitor-1/serpin family E member 1; PAS, periodic acid-Schiff; α -SMA, alpha smooth muscle actin.

This is an open access article under the terms of the [Creative Commons Attribution-NonCommercial](https://creativecommons.org/licenses/by-nc/4.0/) License, which permits use, distribution and reproduction in any medium, provided the original work is properly cited and is not used for commercial purposes.

© 2023 The Authors. *British Journal of Pharmacology* published by John Wiley & Sons Ltd on behalf of British Pharmacological Society.

1 | INTRODUCTION

Kidney transplantation is a life-saving procedure for patients who suffer from end-stage renal disease, which is characterized by severe microalbuminuria and vastly reduced glomerular filtration (Vanhove et al., 2017). Unfortunately, not all patients are eligible for a kidney transplant, as the demand far exceeds the supply (van Leeuwen et al., 2022). On top of that, clinical outcomes of kidney transplantation are not always good, as post-transplant complications are frequently observed. One of the most common post-transplant complications is interstitial fibrosis and tubular atrophy (IF/TA). In fact, this complication is detectable in ~25% of kidney allografts after 1 year and in 90% after 10 years (Saritas & Kramann, 2021). Patients who develop interstitial fibrosis and tubular atrophy eventually must resume dialysis, undergo re-transplantation or suffer from premature death, as the allograft function declines due to the excessive deposition of extracellular matrix (ECM) proteins and loss of tubular epithelial cells. Therefore, safer and more effective treatments for slowing or perhaps even reversing interstitial fibrosis and tubular atrophy are greatly desired.

One approach to reducing the onset of interstitial fibrosis and tubular atrophy is to minimize allograft damage caused by ischaemia-reperfusion injury (IRI). To do so, clinicians are increasingly using machine perfusion, as it is proven superior to static cold storage (Jochmans et al., 2010; Moers et al., 2009). The concept of machine perfusion is based on the controlled flow of a solution, containing nutrients, metabolites and oxygen through an *ex vivo* organ. Besides hypothermic machine perfusion (HMP) that aims to preserve organs, normothermic machine perfusion (NMP) technology has been introduced in the clinics to assess organ function (Hosgood et al., 2018). This technique could also be used as a treatment platform by supplementing perfusion solutions with inhibitors of signalling pathways that regulate fibrogenesis such as **galunisertib**, which is an inhibitor of the **transforming growth factor-beta (TGF- β /TGF β 1)** pathway (van Leeuwen et al., 2022). The TGF β pathway plays a key role in fibrosis because it drives the differentiation of fibroblasts into myofibroblasts, key effector cells that produce large quantities of matrix proteins, especially collagens and fibronectins (Isaka, 2018). For this reason, galunisertib seems to be a promising drug candidate for attenuating fibrosis. When administered systemically, however, this drug can cause potential adverse effects (Huang et al., 2021; Isaka, 2018). Therefore, we devised a new repurposing strategy in which galunisertib is administered *ex vivo*.

In this proof-of-concept study, we investigated the safety and efficacy of this novel therapeutic approach, using a newly developed drug testing platform combining *ex vivo* machine perfusion and tissue slices. We perfused porcine kidneys for 6 h with a blood-based perfusate containing TGF β 1, galunisertib or a combination thereof. To determine whether effects persisted upon ceasing treatments, we also cultured precision-cut tissue slices, prepared from the treated kidneys, for an additional 48 h. Slices are viable explants that can be cultured *ex vivo* for up to a few days, thereby offering an unmatched opportunity to further explore the potential effects of galunisertib on renal

What is already known

- Galunisertib has antifibrotic effects in precision-cut kidney slices.

What does this study add

- Galunisertib shows strong antifibrotic effects in fully isolated kidneys.
- Normothermic machine perfusion can be utilized as a drug delivery platform.

What is the clinical significance

- Drug administration during *ex vivo* perfusion allows for targeted treatment without systemic effects.
- Galunisertib could be used to attenuate interstitial fibrosis and tubular atrophy.

tissue (Bigaeva, Stribos, et al., 2020; Jensen et al., 2019). With respect to read-outs, we focused on analysing the general tissue viability, as well as the release of general injury markers and specific oxidative stress markers during perfusion and in slices. Renal function was assessed during perfusion. We also comprehensively characterized the effect of galunisertib on the extent of inflammation and, more importantly, the onset of fibrogenesis during perfusion and in slices.

2 | METHODS

2.1 | Study design

This study aimed to investigate the antifibrotic effect of galunisertib using a combination of normothermic machine perfusion and precision-cut kidney slices. Extensive pilot studies were performed to optimize our experimental model, study design, and protocol. Exclusion criteria were visibly damaged kidneys (cuts, cysts etc.) or kidneys with aberrant arteries during organ retrieval, insufficient kidney function and technical issues during normothermic machine perfusion, and infections during slice incubation. These criteria were established prospectively. Our primary endpoint was the effect of galunisertib on gene expression of fibrosis-related markers. Investigators were not blinded during the execution of normothermic machine perfusion and slice experiments. However, they were blinded during the execution of all consecutive analyses.

2.2 | Organ procurement and preservation

Animal studies are reported in compliance with the ARRIVE guidelines (Percie du Sert et al., 2020) and with the recommendations made by the *British Journal of Pharmacology* (Lilley et al., 2020). Kidneys were obtained from 6-month-old female Dutch Landrace pigs from a local abattoir in accordance with all guidelines of the Dutch food safety authority. Pigs were anaesthetized by an electrical shock and exsanguinated. After 30 min of warm ischaemia, the kidneys were flushed with ice-cold saline. After cannulation, the kidneys were connected to an hypothermic machine perfusion device (HMP; Kidney Assist Transport, XVIVO, Göteborg, Sweden). Hypothermic machine perfusion was performed for 24 h, at 4°C, using pulsatile pressure-controlled perfusion with a mean arterial pressure of 25 mmHg and 100% oxygenated (100 ml·min⁻¹) University of Wisconsin machine perfusion solution (UW-MP) (Belzer MPS, Bridge to Life, London, UK).

2.3 | Normothermic machine perfusion

After hypothermic machine perfusion, kidneys were flushed with ice-cold saline and cannulated for. Normothermic machine perfusion was carried out using a custom-built perfusion circuit containing an organ chamber, a centrifugal pump (Medos Medizintechnik AG, Radeberg, Germany) controlled by a custom-designed pressure-controlled perfusion machine (LabView Software) set at 80 mmHg with an amplitude of 15, a clinical-grade oxygenator/heat exchanger (Hilite 800 LT, Medos Medizintechnik AG) supplied with carbogen (95% O₂/5% CO₂) at a rate of 0.5 L·min⁻¹, a clinical-grade pressure sensor (Edwards Lifesciences) and an ultra-sensitive flow sensor (Transonic). The total set-up was surrounded by a heating cabinet to keep the temperature stable at 37°C, with the help of temperature sensors and an electric heater (Tristar).

The perfusate contained 835 ml of heparinized leukocyte-depleted autologous whole blood with a haematocrit of 36% and 165 ml of Ringer's solution as well as 10 µg·ml⁻¹ of ciprofloxacin, 0.1% sodium bicarbonate 0.0625% glucose, 8.3 µg·ml⁻¹ of dexamethasone, 10 µg·ml⁻¹ of mannitol, 0.135 µg·ml⁻¹ of creatinine and 2.7 µg·ml⁻¹ of sodium nitroprusside. During normothermic machine perfusion, the perfusate was also supplemented through continuous infusion (20 ml·h⁻¹) of a solution comprising 10% aminoplasmal, 0.25% sodium bicarbonate, 0.2 U·ml⁻¹ of insulin and 35 IE·ml⁻¹ of heparin). After 1 h of normothermic machine perfusion, treatments were started by exposing kidneys to 5 ng·ml⁻¹ of TGF-β (TGFβ1), 10 µM of galunisertib suspended in dimethyl sulfoxide (DMSO) or a combination thereof (TGFβ1 + galunisertib). The perfusate of control kidneys was supplemented with DMSO (0.38%), which served as a vehicle (control). The concentration of galunisertib was previously identified as the most optimal concentration and DMSO as the most optimal solvent (Luangmonkong et al., 2017). In total, the kidneys were treated for 5 h. Urine, perfusate and biopsies were sampled at various time points during normothermic machine perfusion. Urine was recirculated after sampling for a more stable perfusion (Weissenbacher et al., 2019).

2.4 | Precision-cut kidney slices

After normothermic machine perfusion, the kidneys were immediately flushed with ice-cold saline. Cortical tissue cores were subsequently prepared using a biopsy puncher. The tissue cores were transferred to ice-cold UW cold storage solution (Bridge to Life). Slices with a thickness of 300 µm and a diameter of 6 mm were prepared with a Krumdieck tissue slicer (Alabama Research and Development, Munford, AL, USA), as described previously (Bigaeva, Puerta Cavanzo, et al., 2020). Slices were cultured in 12-well plates, containing pre-warmed (37°C) culture medium (1.3 ml per well), at 5% CO₂ and 80% O₂ while being gently shaken (90 cycles·min⁻¹) for 48 h. Culture medium comprised, 10 µg·ml⁻¹ of ciprofloxacin and 0.25 µg·ml⁻¹ of amphotericin B. To determine whether effects persisted upon ceasing treatments, slices were cultured without continuing treatment for 48 h. Culture media were refreshed after 24 h.

2.5 | Cell viability assay

Using a Minibead-beater (2 cycles of 45 s), cortical biopsies and slices (3 replicates per pig) were homogenized in ice-cold sonication solution (70% ethanol and 2 mM of ethylenediaminetetraacetic acid [EDTA]). After centrifugation (16,000 × g at 4°C for 5 min), supernatants were analysed using an **adenosine triphosphate (ATP)** Bioluminescence Kit (Roche Diagnostics, Mannheim, Germany). Supernatants were subsequently stored overnight at 37°C, allowing for the evaporation of sonication solution. The respective pellets were reconstituted, and the resulting supernatants were analysed using a Pierce BCA Protein Assay Kit (Invitrogen). ATP values were normalized to protein content.

2.6 | Lipid peroxidation assay

Culture medium and perfusate samples were analysed to investigate the formation of thiobarbituric acid-reactive substances (TBARS), which are often used as an indicator of oxidative stress, as previously described (Hoeksma et al., 2017). Thiobarbituric acid-reactive substances are shown as delta malondialdehyde (MDA) levels compared with baseline.

2.7 | Evaluation of perfusion parameters

The renal flow rate and urine production were logged during normothermic machine perfusion. Creatinine and sodium concentrations in urine and perfusate samples, lactate dehydrogenase (LDH) and aspartate aminotransferase (ASAT) in perfusate samples, and protein levels in urine samples were analysed in a standardized manner by the clinical chemistry department of the University Medical Center Groningen. Additionally, partial oxygen pressure and haemoglobin content and saturation were measured using an ABL90 FLEX blood

gas analyser (Radiometer, Zoetermeer, the Netherlands). Urinary N-acetyl- β -D-glucosaminidase (NAG) levels were determined as described previously (Findlay et al., 1958). Equations for calculating oxygen consumption, metabolic coupling, creatinine clearance and fractional sodium excretion are shown in Table 1.

2.8 | Histological assessment

Cortical needle biopsies (1.5 mm) and slices (3 slices per pig) were fixed in 4% formalin, after which they were dehydrated by immersing tissues in a series of ethanol solutions of increasing concentrations. The tissues were then cleared in xylene, embedded in paraffin wax and cut into sections of 4 μ m. Sections were stained using a periodic acid-Schiff (PAS) staining to visualize morphological features. Sections were scanned with a C9600 NanoZoomer (Hamamatsu Photonics, Hamamatsu, Japan) to obtain high-resolution digital data. Semi-quantitative scores were assigned to PAS-stained sections in a blinded manner by three individuals, marking glomerular dilatation and structure, tubular dilatation and acute tubular necrosis (Table 2). Scoring of Picro-Sirius red was performed using polarization contrast microscopy, as previously described by Street et al. (2014). In short, areas throughout the tissue were photographed using fluorescence microscopy (Leica, 11888906), after which a positive pixel count was carried out using ImageJ (National Institutes of Health).

2.9 | Gene expression analysis

Total RNA was extracted from 3 mm of cortical needle biopsies and slices (3 slices pooled per pig) using TRIzol reagent (Invitrogen). The yield of extracted RNA was analysed with a NanoDrop 1000 spectrophotometer (NanoDrop Technologies, Wilmington, DE, USA), and the

quality was assessed using RNA electrophoresis. Extracted RNA was reverse transcribed using M-MLV Reverse Transcriptase (Invitrogen) at 37°C for 50 min. Real-time quantitative polymerase chain reaction

TABLE 2 Semi-quantitative histological scoring system.

Glomerular dilation and structural changes	
0	Glomeruli are still intact and demonstrate a clear clove structure. Capillaries have thin walls and are clearly visible.
1	The clove structure is less present, and glomeruli are not entirely intact. Capillaries are less present and dilated, and capillary walls are not clearly visible. Heightened dilatation of the Bowmans space. The Bowmans space can be filled with necrotic tissue/cells.
2	Complete dilatation of the Bowmans space (50%–100% of the glomerulus' size). Glomeruli have decreased in size and are crumpled up.
Tubular dilation	
0	The tubules are not dilated. The brush border and tubular membranes are clearly visible.
1	The tubules are twice their regular size. Intratubular space is visible and tubule membranes are no longer attached to each other. Tubular cells still have a regular size. The brush border is no longer visible.
2	The tubules have increased to more than twice their regular size. The tubular cells are not visible and have irregular shapes.
Acute tubular necrosis	
0	No necrotic tissue visible. The tubules are not dilated. The brush border and tubular membranes are clearly visible.
1	Some necrotic tissue is visible. Little thickening of the membranes, and the tubules contain some cells.
2	Vacuolization of cells, and loss of brush border. Dilation of tubular lumen, and mild interstitial inflammation. The epithelium of the proximal tubules is flattened and simplified. No clear tubular definition. Thickening of the tubule membrane and the tubules contain many cells.

TABLE 1 Equations used for calculating renal function and viability.

Oxygen consumption ($\text{ml O}_2 \cdot \text{min}^{-1} \cdot 100 \text{ g}^{-1}$)

$$\text{Hb} = 0.024794 * (100 - \text{SO}_2 \text{ venous}) + K * (\text{pO}_2 \text{ arterial} - \text{pO}_2 \text{ venous}) * Q * 100$$

Metabolic coupling ($\text{mmol Na} \cdot \text{mmol O}_2^{-1} \cdot 100 \text{ g}^{-1}$)

$$0.001 * \frac{(\text{eGFR} * \text{P}_{\text{Na}}) - (U * U_{\text{Na}})}{\text{O}_2} * 100$$

Creatinine clearance ($\text{ml} \cdot \text{min}^{-1} \cdot 100 \text{ g}^{-1}$)

$$\left(\frac{U_{\text{Cr}} * U}{P_{\text{Cr}}} \right) * 100$$

Fractional sodium excretion (%)

$$100 * \frac{U_{\text{Na}} * P_{\text{Cr}}}{P_{\text{Na}} * U_{\text{Cr}}}$$

Hb: Haemoglobin content ($\text{mmol} \cdot \text{L}^{-1}$).

pO₂: Partial oxygen pressure (kPa).

K: Solubility constant of oxygen in H₂O at 37°C (0.0225 $\text{ml O}_2 \cdot \text{kPa}^{-1}$).

SO₂: Haemoglobin saturation (%).

Q: Renal blood flow ($\text{L} \cdot \text{min}^{-1}$).

g: Kidney weight (gram).

eGFR: Creatinine clearance.

P_{Na}: Perfusate sodium concentration ($\text{mmol} \cdot \text{L}^{-1}$).

U: Urine production rate ($\text{ml} \cdot \text{min}^{-1}$).

U_{Na}: Urine sodium concentration ($\text{mmol} \cdot \text{L}^{-1}$).

O₂: Oxygen consumption ($\text{ml O}_2 \cdot \text{min}^{-1}$).

g: Kidney weight (gram).

U_{Cr}: Urine creatinine concentration ($\text{mmol} \cdot \text{L}^{-1}$).

U: Urine production rate ($\text{ml} \cdot \text{min}^{-1}$).

P_{Cr}: Perfusate creatinine concentration ($\text{mmol} \cdot \text{L}^{-1}$).

g: Kidney weight (gram).

U_{Na}: Urine sodium concentration ($\text{mmol} \cdot \text{L}^{-1}$).

P_{Na}: Perfusate sodium concentration ($\text{mmol} \cdot \text{L}^{-1}$).

P_{Cr}: Perfusate creatinine concentration ($\text{mmol} \cdot \text{L}^{-1}$).

U_{Cr}: Urine creatinine concentration ($\text{mmol} \cdot \text{L}^{-1}$).

(qPCR) was conducted using specific primers (Table 3), Taq DNA Polymerase (Invitrogen) and a Quant Studio 7 Flex qPCR machine (Applied Biosystems, Bleiswijk, the Netherlands), which was configured with 1 cycle of 10 min at 95°C and 40 consecutive cycles of 15 s at 95°C and 1 min at 60°C. CT-values were corrected for *Actb* levels (that did not differ between groups). The fold induction is presented as $2^{-\Delta\Delta C_t}$, with the mean of all samples per time point set to 1.

2.10 | Interleukin-6 (IL-6) immunoassay

The Immuno-related procedures used comply with the recommendations made by the *British Journal of Pharmacology* (Alexander et al., 2018). IL-6 was measured as it is strongly associated with the onset of fibrosis (Li et al., 2022). Culture medium and perfusate samples were analysed with a Porcine IL-6 Duo Set enzyme-linked immunosorbent assay (ELISA) (Bio-Techne, Abingdon, UK), according to the manufacturer's instructions.

2.11 | Data and statistical analysis

The experiments were designed to use groups of equal size using randomization. GraphPad Prism (Version 8.4.2.) was used to visualize and analyse the data. All data are expressed as aligned scatter plots and/or the arithmetic mean with the standard error of the mean (SEM). For longitudinal data, differences across all experimental groups were assessed using a two-way analysis of variance (ANOVA) with the Geisser–Greenhouse correction followed by Tukey's multiple comparisons. Single time points were analysed using a one-way ANOVA followed by Fisher's least significant difference test. All statistical tests were two-tailed, and differences between groups were considered statistically significant when $P < 0.05$. In multigroup studies with parametric variables, post hoc tests were conducted only if F achieved $P < 0.05$ and there was no significant variance in homogeneity. Normality was tested and unwanted sources of variation were reduced by data normalization. Only one kidney (both left and right kidneys) from each pig was used and randomized into experimental groups. The

sample size of $n = 8$ per experimental group was determined based on preliminary experiments (van Leeuwen et al., 2023). For each analysis requiring tissues, three tissue slices were incubated per kidney but pooled for the analysis. The group size is the number of independent values, and statistical analyses were performed using these independent values. Unpaired statistical analyses were therefore applied. Heterogeneity among animals was expected as the pigs were not bred in a standardized manner. The data and statistical analysis comply with recommendations of the *British Journal of Pharmacology* on experimental design and analysis in pharmacology (Curtis et al., 2022).

2.12 | Materials

Sodium bicarbonate, aminoplasmal and sodium bicarbonate were purchased from B. Braun (Melsungen, Germany), while glucose, Ringer's solution and mannitol were obtained from Baxter (Utrecht, the Netherlands). Dexamethasone was purchased from Centrafarm, (Etten-Leur, the Netherlands), while creatinine and sodium nitroprusside were purchased from Merck (address). Insulin was obtained from Novo Nordisk (Bagsvaerd, Denmark) and heparin from Leo Pharma (Ballerup, Denmark). TGFβ1 (TGF-β) was purchased Sigma Aldrich, (Amsterdam, the Netherlands), while galunisertib was purchased from Axon Medchem (Groningen, the Netherlands). William's Medium E and GlutaMAX and ciprofloxacin were obtained from Invitrogen (Landsmeer, the Netherlands). Ethanol and ethylenediaminetetraacetic acid [EDTA]) were purchased from Merck (Darmstadt, Germany) while ciprofloxacin and amphotericin B from Merck (Darmstadt, Germany). Details of other materials and suppliers are provided in the specific sections.

2.13 | Nomenclature of targets and ligands

Key protein targets and ligands in this article are hyperlinked to corresponding entries in the IUPHAR/BPS Guide to PHARMACOLOGY <http://www.guidetopharmacology.org> and are permanently archived in the Concise Guide to PHARMACOLOGY 2021/22 (Alexander et al., 2021).

Gene	Forward sequence (5' → 3')	Reverse sequence (5' → 3')
<i>Acta2</i>	ACGAAGCCCCAAGCAAAAGA	GTTGGTGATGATGCCGTGTTC
<i>Actb</i>	TCTGCGCAAGTTAGGTTTTGTC	CGTCCACCGCAAATGCTT
<i>Col1a2</i>	CAAGAAAGGGCCCAACTGGA	AGGGCCTGGGATACCATCAT
<i>Fn1</i>	GCACCATCCAACCTTGCGTTT	TGTACTCGGTTGCTGGTTCC
<i>Ilib</i>	GATGACACGCCACCCCTG	CAAATCGCTTCTCCATGTCCC
<i>Il6</i>	AGACAAAGCCACCACCCCTAA	CTCGTTCTGTGACTGCAGCTTATC
<i>Serpine1</i>	GCAAGTTCGGGCTCCACTAC	TGCATGCCGTAACCTCCTG
<i>Serpinh1</i>	TGCAGTCCATCAACGAGTGG	TGGAATCGCTCATCCCAGTG
<i>Tgfb1</i>	GGGAGGGTGTTTCATGGTAGGA	AGCTCACCCCAAATTCATCTTC
<i>Tnf</i>	GGTGCCTTGTTTCAGATGT	CAGGTGGGAGCAACCTACAGTT

TABLE 3 Primer sequences.

3 | RESULTS

3.1 | Set-up of an ex vivo renal transplant and fibrogenesis model

Our integrated ex vivo model, optimal for drug delivery, was based on state-of-the-art machine perfusion techniques combined with the use of precision-cut tissue slices (Figure 1a). We obtained porcine kidneys, with an average weight of 365 ± 36 g, from a local abattoir and subjected them to 30 min of warm ischaemia to reflect conditions of deceased donation. The kidneys were then transported and preserved for 24 h using oxygenated hypothermic machine perfusion, using a mean arterial pressure of 25 mmHg and a temperature of $3.8 \pm 1.2^\circ\text{C}$ (Figure 1b). During hypothermic machine perfusion,

the flow rate ranged between 25 and $70\text{ ml}\cdot\text{min}^{-1}$ and increased over time. We subsequently performed normothermic machine perfusion using a custom-built set-up, configured with a mean arterial pressure of 80 mmHg and a temperature of $37 \pm 1.3^\circ\text{C}$ (Figure 1c). Kidneys were subjected to 1 h of normothermic machine perfusion before adding treatments to the perfusate (i.e. TGF β 1, galunisertib or a combination thereof). TGF β 1 was added to the perfusate to stimulate fibrogenesis. During normothermic machine perfusion, the flow rate ranged from 200 to $500\text{ ml}\cdot\text{min}^{-1}$. The renal flow rate was significantly lower for kidneys perfused with TGF β 1 as compared with other groups. After normothermic machine perfusion, the perfused kidney tissue was used for the preparation of slices. This was performed to establish whether potential effects persisted upon ceasing treatments.

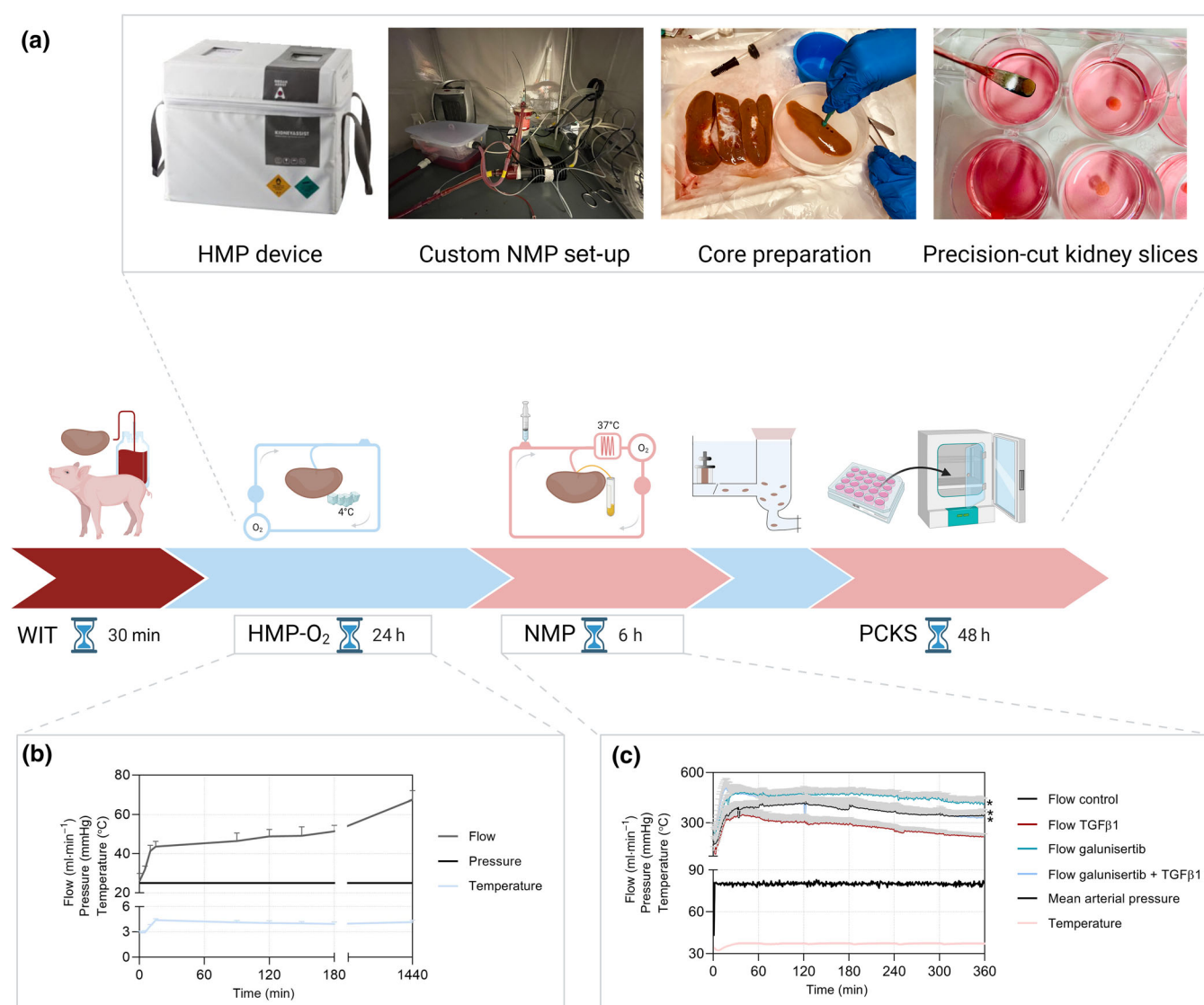


FIGURE 1 Machine perfusion and organ slices workflow as a platform for ex vivo drug delivery. (a) Porcine kidneys were subjected to 30 min of warm ischaemia, 24 h of oxygenated hypothermic machine perfusion (HMP) and 6 h of normothermic machine perfusion (NMP) with treatment, after which slices were prepared from the respective kidneys and incubated for an additional 48 h. (b) Perfusion parameters during oxygenated HMP (n = 32 kidneys obtained from 32 pigs), and (c) perfusion parameters during NMP (n = 8 kidneys per group). *P < 0.05. Values are expressed as mean \pm SEM. PCKS, precision-cut kidney slices; TGF β 1, transforming growth factor-beta 1; WIT, warm ischaemia time.

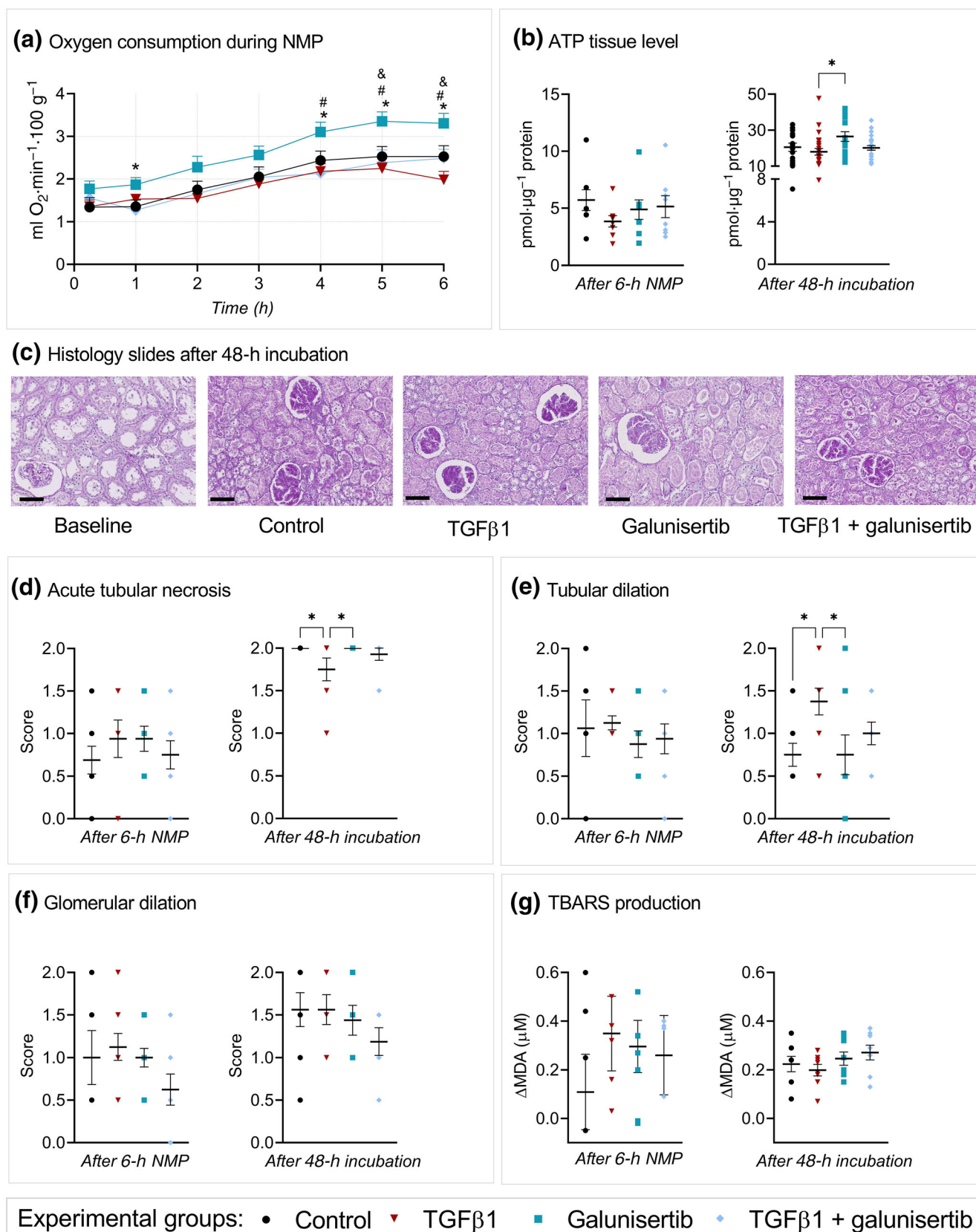


FIGURE 2 Legend on next page.

3.2 | Galunisertib promoted cell viability during normothermic machine perfusion and in slices

Using our novel platform, we first examined whether TGF β 1, galunisertib or a combination thereof compromised cell viability during normothermic machine perfusion and persisted during 48 h of incubation (Figure 2). To that end, we analysed oxygen consumption and ATP levels, as well as general morphological features using a PAS staining. Potential effects on oxidative stress were explored by measuring levels of thiobarbituric acid-reactive substances. We observed that galunisertib significantly increased oxygen consumption during the second half of normothermic machine perfusion (Figure 2a). ATP levels, however, were not affected during normothermic machine perfusion but were significantly increased after 48 h when treated with galunisertib during normothermic machine perfusion (Figure 2b). ATP levels after 48 h were much higher than after 6 h of normothermic machine perfusion, indicating that tissue remained viable during incubation. Blinded histological scoring of PAS-stained sections was performed (Figure 2c), and scoring revealed that kidneys had already sustained injury after 6 h of normothermic machine perfusion, as indicated by scores reflecting tubular necrosis (Figure 2d) and dilation (Figure 2e), as well as glomerular dilation (Figure 2f). Treatments produced no adverse effects during normothermic machine perfusion. In slices, the extent of glomerular dilation and tubular necrosis increased after an incubation of 48 h. TGF β 1 treatment during normothermic machine perfusion significantly exacerbated tubular dilation but attenuated acute tubular necrosis in slices after 48 h. We detected no significant differences in thiobarbituric acid-reactive substances levels after 6 h of normothermic machine perfusion and in slices, regardless of treatments used (Figure 2g).

3.3 | Galunisertib did not negatively affect renal function

We subsequently assessed whether renal function was affected by the tested treatments (Figure 3). At various time points during normothermic machine perfusion, samples were collected and analysed to determine urine production, creatinine clearance, fractional sodium excretion and metabolic coupling. We observed that there were no significant differences in urine production between the groups and urine production also remained stable over time, with only a minor and temporary decline at 1 h (Figure 3a). In comparison with the control, kidneys treated with only TGF β 1 seemed to have a reduced clearance of creatinine, albeit not significantly (Figure 3b). The fractional sodium excretion after 1 h of normothermic machine perfusion,

however, was significantly different between TGF β 1 only and TGF β 1 + galunisertib groups (Figure 3c). In addition, the fractional sodium excretion decreased during the first hour of normothermic machine perfusion, after which it remained stable. With respect to metabolic coupling, we observed no significant differences between controls and treatments (Figure 3d).

3.4 | Galunisertib did not cause additional damage during normothermic machine perfusion

To establish whether treatments caused additional damage during normothermic machine perfusion, we measured lactate dehydrogenase and aspartate aminotransferase levels in perfusate, as well as total protein and N-acetyl- β -D-glucosaminidase content in urine (Figure 4). The release of lactate dehydrogenase into the perfusate, which marks cell damage, increased over time, levelling off around the 3-h time point, but remained unaffected by TGF β 1, galunisertib or a combination thereof (Figure 4a). Similar observations were made for aspartate aminotransferase levels in the perfusate, which were used as a marker for mitochondrial damage (Figure 4b). The total amount of excreted protein, indicating proteinuria, increased linearly over time and remained unaffected by the tested treatments (Figure 4c). Likewise, the total amount of urinary N-acetyl- β -D-glucosaminidase, indicating tubular injury, increased during normothermic machine perfusion and was not significantly different among the experimental groups (Figure 4d).

3.5 | Galunisertib affected inflammation during normothermic machine perfusion and in slices

After confirming that galunisertib did not affect cell viability and renal function, we analysed mRNA expression of *Il1b*, *Tgfb1*, *TFNA* (*TFN*) and *Il6*, as well as IL-6 protein content to identify potential effects on inflammation (Figure 5). We found that *Il1b* mRNA expression in kidneys treated with TGF- β 1 and galunisertib was significantly lower after normothermic machine perfusion than the control and those treated with TGF- β 1 (Figure 5a). After 48 h of incubation, treatment-dependent effects on *Il1b* (interleukin-1 beta gene) mRNA expression diminished. Similar observations were made for *Tgfb1* mRNA expression, which was significantly reduced after 6 h of normothermic machine perfusion when treated with galunisertib and TGF- β 1 compared with kidneys treated with just galunisertib or TGF β 1 (Figure 5b). This effect changed after 48 h of incubation, as the galunisertib-treated group showed significantly lower *Tgfb1* mRNA expression

FIGURE 2 Galunisertib does not affect general viability. As shown by the (a) oxygen consumption (#: significance between transforming growth factor-beta 1 [TGF β 1] and galunisertib, *: significance between galunisertib and TGF β 1 + galunisertib and &: significance between control and galunisertib), (b) adenosine triphosphate (ATP)/protein content in the renal tissue, (c) general morphology visualized using periodic acid-Schiff (PAS) staining (representative images are shown of slices after 48 h of incubation, scale bar = 80 μ m, 26 \times magnification), (d) acute tubular necrosis scores (0–2), (e) tubular dilation scores (0–2), (f) glomerular integrity scores (0–2) and (g) thiobarbituric acid-reactive substances (TBARS) content in perfusate. * P < 0.05. Values are expressed as mean \pm SEM (n = 8 kidneys or 3 \times 8 slices per group). NMP, normothermic machine perfusion; Δ MDA, delta malondialdehyde.

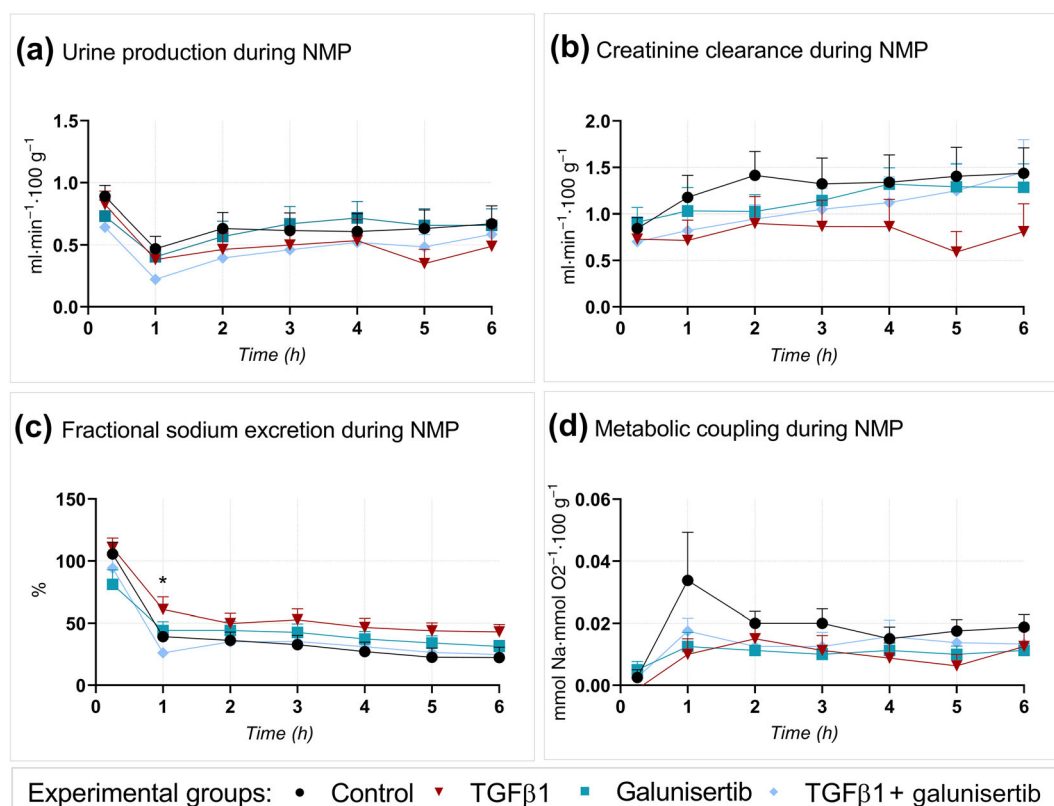


FIGURE 3 Renal function during normothermic machine perfusion (NMP). As shown by (a) the urine production rate, (b) the creatinine clearance, (c) the fractional sodium excretion and (d) the metabolic coupling. * $P < 0.05$ between transforming growth factor-beta 1 (TGFβ1) and TGFβ1 + galunisertib. Values are expressed as mean \pm SEM ($n = 8$ kidneys).

levels compared with all other groups. Effects on *Tnfa* (*Tnf*) mRNA expression were also detected after normothermic machine perfusion; galunisertib significantly increased its expression, whereas a combination of TGF-β1 and galunisertib reduced its expression (Figure 5c). The effects reduced after 48 h of incubation. After 6 h of normothermic machine perfusion, *Il6* mRNA expression in kidneys treated with TGFβ1 and galunisertib was significantly lower than the control group and those treated with TGFβ1 alone (Figure 5d). These effects diminished after 48 h of incubation. IL-6 protein levels in the perfusate showed similar trends to IL-6 mRNA expression during 6 h of normothermic machine perfusion (Figure 5e).

To observe the effects of continued treatment on inflammation, slices were incubated for 48 h with the same treatment as during normothermic machine perfusion. These results revealed stronger treatment effects on the mRNA expression of *Tgfb1* and *Tnfa* (Figure S1).

3.6 | Galunisertib attenuated fibrogenesis during normothermic machine perfusion and in slices

To determine whether galunisertib attenuated fibrogenesis—our main research question—we analysed mRNA expression of *Acta2*, *Col1a2*, *Fn1*, *Serpine1* and *Serpinh1* (Figure 6). The expression of *Acta2* mRNA was not affected by treatments after 6 h of normothermic machine perfusion (Figure 6a). After 48 h of incubation, however, mRNA

expression of *Acta2* was significantly reduced when treated with galunisertib compared with slices treated with TGFβ1 or treated with galunisertib and TGFβ1. *Col1a2* mRNA expression was also significantly reduced after 48 h of incubation for the galunisertib-treated group (Figure 6b). No significant effects on *Fn1* mRNA expression were observed (Figure 6c). Interestingly, *Serpine1* mRNA expression was already significantly reduced in kidneys perfused with galunisertib after 6 h of normothermic machine perfusion, and this effect was still visible after 48 h of incubation (Figure 6d). With respect to *Serpinh1* mRNA expression, reductions were only observed after 6 h of normothermic machine perfusion with TGFβ1 and galunisertib (Figure 6e). Sirius red staining revealed no significant differences between experimental groups after both 6 h of normothermic machine perfusion and 48 h of incubation.

To observe the effects of continued treatment on fibrogenesis, slices were incubated for 48 h with the same treatment as during normothermic machine perfusion. These results revealed stronger antifibrotic effects on the mRNA expression of *Acta2*, *Col1a2*, *Fn1* and *Serpine1* when treated with galunisertib (Figure S2).

4 | DISCUSSION

Interstitial fibrosis and tubular atrophy are the main causes of long-term graft loss and a great burden for renal transplant recipients

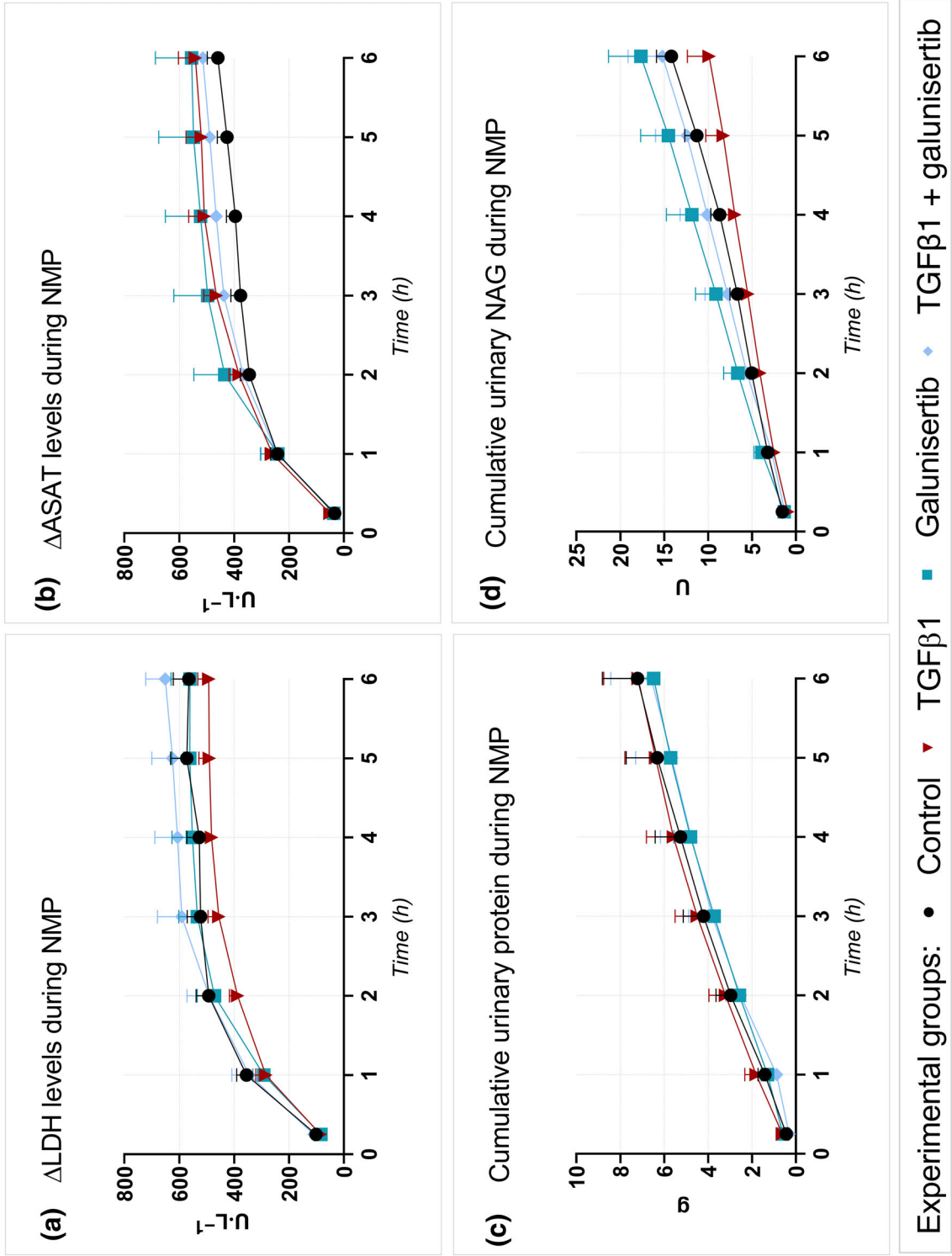


FIGURE 4 Kidney injury during normothermic machine perfusion (NMP) not aggravated by galunisertib. As shown by (a) delta lactate dehydrogenase (Δ LDH) levels in the perfusate, (b) delta aspartate aminotransferase (Δ ASAT) levels in the perfusate, (c) total urinary protein levels and (d) total urinary *N*-acetyl- β -D-glucosaminidase (NAG) levels. Values are expressed as the mean \pm SEM ($n = 8$ kidneys per group). TGF β 1, transforming growth factor-beta 1.

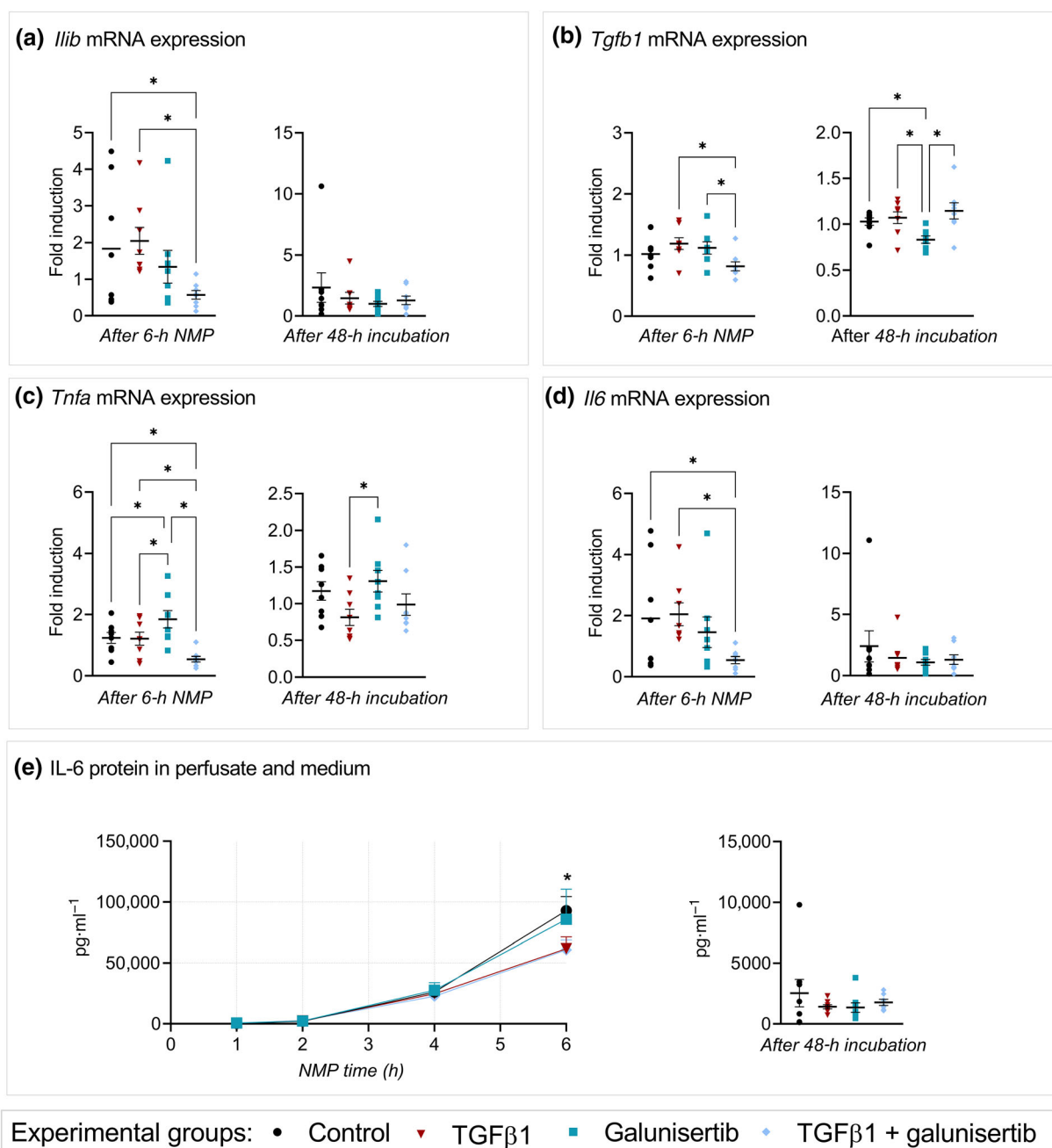


FIGURE 5 Inflammation markers after 6 h of normothermic machine perfusion (NMP) and after 48 h of incubation. As shown by (a) *Il1b* mRNA expression, (b) *Tgfb1* mRNA expression, (c) *Tnfa* mRNA expression, (d) *Il6* mRNA expression and (e) interleukin-6 (IL-6) protein levels in perfusate. * $P < 0.05$ between transforming growth factor-beta 1 (TGFβ1) and TGFβ1 + galunisertib. Fold induction shown as $2^{-\Delta\Delta C_t}$. Values are expressed as the mean \pm SEM ($n = 8$ kidneys or 3×8 slices per group). * $P < 0.05$.

(Cosio et al., 2005; Dinis et al., 2014; Matas et al., 2008). There are currently no safe and effective therapies for halting the onset of fibrosis in kidney allografts. We, therefore, devised a novel repurposing strategy for galunisertib using machine perfusion. We demonstrated that galunisertib suppresses the onset of fibrosis in kidney allografts without compromising renal viability, functionality and injury as assessed by oxygen consumption, tissue ATP levels, histological structure, lipid peroxidation, urine production, proteinuria, creatinine clearance, fractional sodium excretion, metabolic coupling, urinary N-

acetyl-β-D-glucosaminidase, lactate dehydrogenase and aspartate aminotransferase levels.

As galunisertib is a potent inhibitor of the TGFβ1 signalling pathway (Isaka, 2018), one of the main concerns of systemic inhibition of TGFβ signalling is the interference with beneficial biological processes, leading to adverse effects (Huang et al., 2021). Furthermore, the effects of TGFβ1 up-regulation during renal transplantation have shown contradictory results (Du, 2011). Although we could not measure systemic effects of galunisertib in our isolated perfusion model,

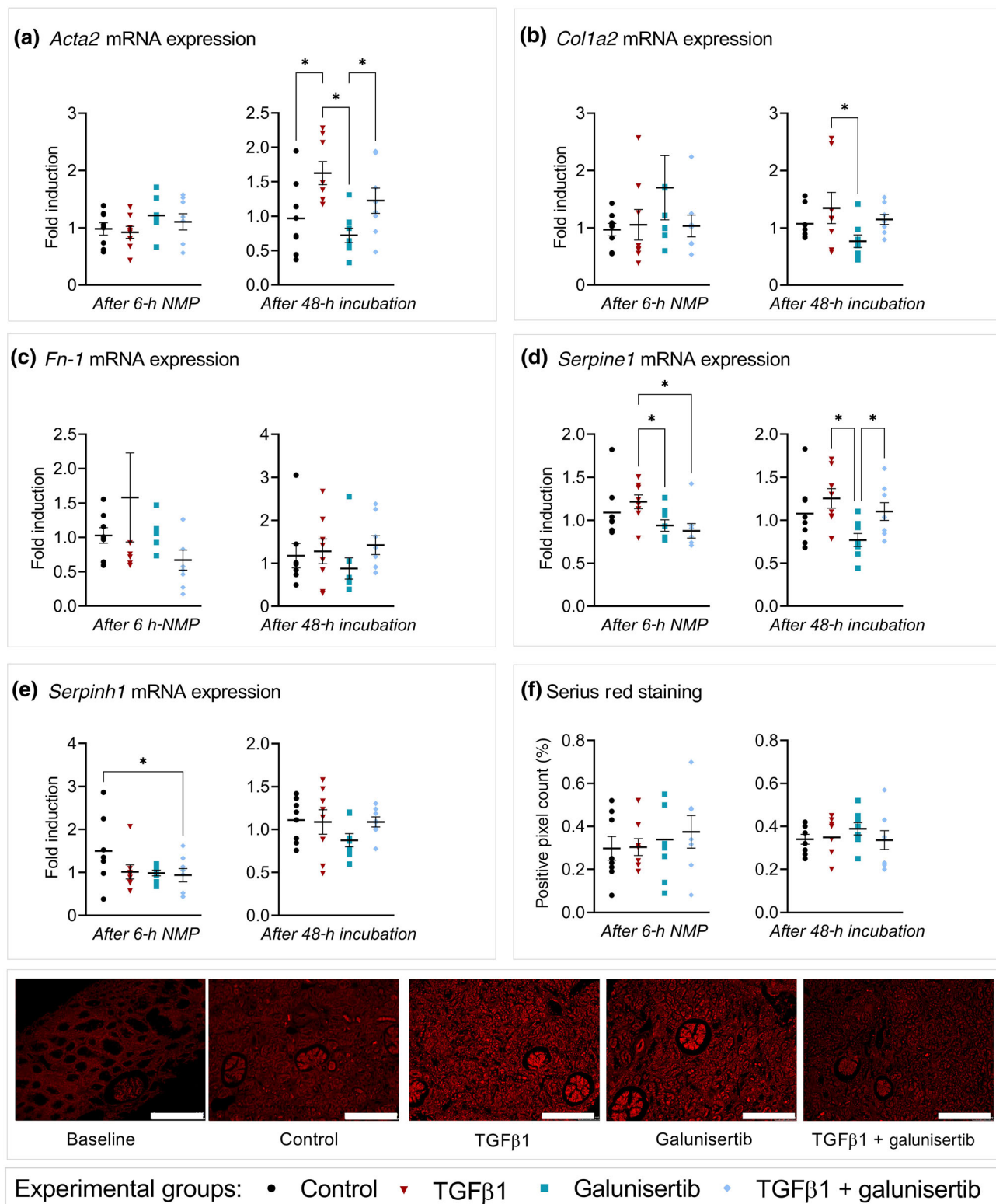


FIGURE 6 Galunisertib attenuates fibrogenesis during normothermic machine perfusion (NMP) and in slices. As shown by (a) *Acta2* mRNA expression, (b) *Col1a2* mRNA expression, (c) *Fn1* mRNA expression, (d) *Serpine1* mRNA expression, (e) *Serpinh1* mRNA expression and (f) Picro-Sirius red staining scored by positive pixel count and slides (scale bar = 250 μ m in a 12 \times magnification). * $P < 0.05$. Fold induction shown as $2^{-\Delta\Delta C_t}$. Values are expressed as the mean \pm SEM ($n = 8$ kidneys or 3×8 slices per group). TGF β 1, transforming growth factor-beta 1.

we did analyse the effects of galunisertib on renal function, injury and viability, of which none were compromised. In fact, galunisertib resulted in a higher oxygen consumption during normothermic machine perfusion and significantly higher ATP levels after 48 h of incubation. Elevated ATP levels have not been previously observed in slices (Bigaeva, Gore, & Mutsaers, 2020; Bigaeva, Puerta Cavanzo, et al., 2020; Luangmonkong et al., 2017). We speculate that these high ATP levels are due to improved cellular respiration during normothermic machine perfusion or the fact that galunisertib is a competitive inhibitor for ATP-binding site of the TGF β 1 (Yingling et al., 2018). Not to forget, fibrogenesis requires an increased energy demand for fibroblast proliferation and protein synthesis (Wang et al., 2022), a process that is suppressed by galunisertib.

TGF- β signalling also plays an important role in suppressing an immune reaction, and galunisertib has demonstrated to block TGF β 1-mediated reduction of naive T-cell proliferation and Treg-mediated suppression of naive T-cells (Holmgaard et al., 2018). As the delicate balance between immunosuppression and immunocompetence plays a crucial role in renal transplant recipients, we analysed the inflammatory effects of galunisertib on an mRNA level. As previously observed, we detected higher expression of tumour necrosis factor- α (TNF- α) gene expression after treatment with galunisertib (Hira et al., 2020). However, galunisertib combined with TGF- β treatment reduced TNF- α expression. We observed significantly lower IL-6 levels after 6 h of normothermic machine perfusion on both mRNA and protein levels, as also observed in a previous study looking into the effects of galunisertib on acute pancreatitis (Liu et al., 2016), suggesting general anti-inflammatory effects. IL-6 is a pro-inflammatory cytokine that plays a fundamental role in immune regulation and tissue homeostasis. Disruptions in IL-6 levels can contribute to the development of acute and chronic rejection of renal allografts (Miller & Madsen, 2021).

Our main aim was to assess the antifibrotic effects of galunisertib. Therefore, we examined mRNA expression of fibrogenesis-related genes, as changes in mRNA expression precede those on protein level. Galunisertib exhibited clear attenuation of *Tgfb1*, *Acta2*, *Col1a2*, *Fn1*, *Serpine1* and *Serpinh1*, which are genes encoding for TGF β 1, alpha smooth muscle actin (α -SMA), fibronectin (*Fn1*), collagen alpha-2(I) chain (*Col1a2*), heat shock protein 47 (HSP47) and plasminogen activator inhibitor-1 (PAI-1/SERPINE 1), after 48 h of incubation. The effects were most profound with continued treatment in slices (Figures S1 and S2), indicating that a longer exposure to galunisertib increases the antifibrotic effects. During fibrogenesis, TGF β triggers a whole cascade of processes such as α -SMA expression by activated myofibroblasts to restore tissue integrity by producing and secreting extracellular matrix proteins, especially collagens and fibronectins (LeBleu et al., 2013), and secretion of the collagen chaperone HSP47 (Razzaque et al., 2005). Similar effects on gene expression of fibrosis markers were observed in previous studies using human, porcine and murine tissue slices (Bigaeva, Gore, & Mutsaers, 2020; Bigaeva, Puerta Cavanzo, et al., 2020; van Leeuwen et al., 2023), although the kidneys described in these studies were not subjected to normothermic machine perfusion.

The galunisertib concentration used, 10 μ M, is in line with other *ex vivo* studies (Bigaeva, Gore, & Mutsaers, 2020; Bigaeva, Puerta Cavanzo, et al., 2020; Luangmonkong et al., 2017). In *vivo*, a much lower dosage, resulting in a C_{\max} of 2–6 μ M, is administered to limit systemic side effects (Rodón et al., 2015; Yingling et al., 2018). By treating an isolated kidney, these adverse effects are circumvented and, therefore, a higher concentration can be used, resulting in more prominent effects. To our knowledge, galunisertib or any other antifibrotic molecule has never before been administered to an isolated metabolically active kidney. The galunisertib was resuspended in DMSO as this is the most suitable solvent. As each group contained 0.38% of DMSO, potential changes caused by DMSO should be similar in all groups (Verheijen et al., 2019).

Although this study provides valuable insights into the value of machine perfusion for delivering drugs in a transplant setting and thereby reducing systemic side effects, there are limitations. In this study, for instance, we were not able to determine long-term effects *in vivo*. This would be a valuable next step to determining whether the proposed strategy reduces interstitial fibrosis and tubular atrophy. Additionally, we did not transplant these kidneys; thus, the graft rejection rate and immunological factors could not be measured. A porcine transplantation study would therefore be a necessary follow-up.

Nevertheless, experimental normothermic machine perfusion models are commonly used platforms for optimizing the resuscitation technique itself, and *ex vivo* renal function accurately reflects the condition of the kidney (Venema et al., 2019, 2021; Weissenbacher et al., 2019). In contrast to renal function, we were able to assess renal mitochondrial activity for an additional 48 h using the well-established technique of precision-cut kidney slices (Bigaeva, Stribos, et al., 2020; van Furth et al., 2022; Jensen et al., 2019; van Leeuwen et al., 2022; Stribos et al., 2016; Tingskov et al., 2021; Vaughan et al., 2022). Kidneys are well-known consumers of oxygen to facilitate oxidative phosphorylation for the active reabsorption of sodium in the tubular cells (Balaban, 1990; Lassen et al., 1961; Singh et al., 2013). Therefore, the renal metabolic state is a valid representation of kidney health (Bellini et al., 2019). As the kidney proximal tubule cells are dependent on the oxidative mitochondrial metabolism, they are particularly prone to harmful effects of mitochondrial damage during ischaemia-reperfusion injury (Kezic et al., 2016; Tan et al., 2013).

Furthermore, this unique *ex vivo* model captures the full complexity of a metabolically active isolated organ, the tissue architecture and cell-cell and cell-matrix interactions, which are vital to consider in fibrosis research (Frangogiannis, 2016). Pretreatment with TGF β 1 is an effective method to enhance the onset of fibrosis in a relative brief period of time. Additionally, the great advantage of using porcine kidneys obtained from the abattoir is that they are, genetically, physiologically and heterogeneity wise, similar to human kidneys (Porrett et al., 2022), and limit the use of laboratory animals. However, inter-species differences remain.

This technique can be used to answer all sorts of transplant-related questions, for example to optimize normothermic machine perfusion conditions with a more extended read-out period or to study the complexities of brain death, ischaemia, reperfusion,

fibrogenesis and the onset of fibrosis. Not to forget, this platform could be implemented using human tissue for more translational results and other organs, such as lungs, hearts and livers.

The current proof-of-concept study demonstrates the value of repurposing potent antifibrotic drugs for treating fibrosis in a renal transplant setting using *ex vivo* machine perfusion. With further research using transplant models, discarded human kidneys and clinical evaluation, we envision that small molecule drugs such as galunisertib could provide the aid to renal allograft-related interstitial fibrosis and tubular atrophy.

AUTHOR CONTRIBUTIONS

L. Leonie van Leeuwen: Conceptualization (equal); data curation (lead); formal analysis (equal); methodology (equal); visualization (lead); writing—original draft (equal); writing—review and editing (equal). **Mitchel J. R. Ruigrok:** Conceptualization (equal); methodology (equal); writing—original draft (supporting); writing—review and editing (equal). **Benedikt M. Kessler:** Conceptualization (equal); supervision (equal); writing—review and editing (equal). **Henri G. D. Leuvenink:** Conceptualization (equal); methodology (equal); supervision (equal); writing—review and editing (equal). **Peter Olinga:** Conceptualization (equal); methodology (equal); supervision (equal); writing—review and editing (equal).

ACKNOWLEDGEMENTS

The authors are incredibly grateful for abattoir Kroon Vlees for their collaboration and providing the kidneys for this research. Many thanks to Yvette Jansen, Danique Zantinge, Meindert Tangerman, Petra Ottens and Janneke Wiersema-Buist for their assistance with execution of the experiments and analyses.

CONFLICT OF INTEREST STATEMENT

The authors declare no conflicts of interest.

DATA AVAILABILITY STATEMENT

Data are available on request from the authors.

DECLARATION OF TRANSPARENCY AND SCIENTIFIC RIGOUR

This Declaration acknowledges that this paper adheres to the principles for transparent reporting and scientific rigour of preclinical research as stated in the *BJP* guidelines for [Design and Analysis](#), [Immunoblotting and Immunochemistry](#) and [Animal Experimentation](#), and as recommended by funding agencies, publishers and other organizations engaged with supporting research.

ORCID

L. Leonie van Leeuwen  <https://orcid.org/0000-0003-4666-2993>

Mitchel J. R. Ruigrok  <https://orcid.org/0000-0002-6267-9640>

Benedikt M. Kessler  <https://orcid.org/0000-0002-8160-2446>

Henri G. D. Leuvenink  <https://orcid.org/0000-0001-5036-2999>

Peter Olinga  <https://orcid.org/0000-0003-4855-8452>

REFERENCES

- Alexander, S. P., Christopoulos, A., Davenport, A. P., Kelly, E., Mathie, A., Peters, J. A., Veale, E. L., Armstrong, J. F., Faccenda, E., Harding, S. D., Pawson, A. J., Southan, C., Davies, J. A., Abbracchio, M. P., Alexander, W., Al-hosaini, K., Bäck, M., Barnes, N. M., Bathgate, R., ... Ye, R. D. (2021). THE CONCISE GUIDE TO PHARMACOLOGY 2021/22: G protein-coupled receptors. *British Journal of Pharmacology*, 178(S1), S27–S156. <https://doi.org/10.1111/bph.15538>
- Alexander, S. P. H., Roberts, R. E., Broughton, B. R. S., Sobey, C. G., George, C. H., Stanford, S. C., Cirino, G., Docherty, J. R., Giembycz, M. A., Hoyer, D., Insel, P. A., Izzo, A. A., Ji, Y., MacEwan, D. J., Mangum, J., Wonnacott, S., & Ahluwalia, A. (2018). Goals and practicalities of immunoblotting and immunohistochemistry: A guide for submission to the *British Journal of Pharmacology*. *British Journal of Pharmacology*, 175(3), 407–411. <https://doi.org/10.1111/bph.14112>
- Balaban, R. S. (1990). Regulation of oxidative phosphorylation in the mammalian cell. *American Journal of Physiology. Cell Physiology*, 258(3), 27–23. <https://doi.org/10.1152/ajpcell.1990.258.3.C377>
- Bellini, M. I., Yiu, J., Nozdrin, M., & Papalouis, V. (2019). The effect of preservation temperature on liver, kidney, and pancreas tissue ATP in animal and preclinical human models. *Journal of Clinical Medicine*, 8(9), 1421. <https://doi.org/10.3390/jcm8091421> <https://pubmed.ncbi.nlm.nih.gov/31505880/>. Accessed January 11, 2022
- Bigaeva, E., Gore, E., & Mutsaers, H. A. M. (2020). Exploring organ-specific features of fibrogenesis using murine precision-cut tissue slices. *Biochimica et Biophysica Acta, Molecular Basis of Disease*, 1866(1), 165582. <https://doi.org/10.1016/j.bbdis.2019.165582> <https://pubmed.ncbi.nlm.nih.gov/31676376/>. Accessed February 5, 2021
- Bigaeva, E., Puerta Cavanzo, N., Stribos, E. G. D., de Jong, A. J., Biel, C., Mutsaers, H. A. M., Jensen, M. S., Nørregaard, R., Leliveld, A. M., de Jong, I. J., Hillebrands, J. L., van Goor, H., Boersema, M., Bank, R. A., & Olinga, P. (2020). Predictive value of precision-cut kidney slices as an *ex vivo* screening platform for therapeutics in human renal fibrosis. *Pharmaceutics*, 12(5), 459. <https://doi.org/10.3390/pharmaceutics12050459>
- Bigaeva, E., Stribos, E. G. D., Mutsaers, H. A. M., Piersma, B., Leliveld, A. M., de Jong, I. J., Bank, R. A., Seelen, M. A., van Goor, H., Wollin, L., Olinga, P., & Boersema, M. (2020). Inhibition of tyrosine kinase receptor signaling attenuates fibrogenesis in an *ex vivo* model of human renal fibrosis. *American Journal of Physiology*, 318(1), F117–F134. <https://doi.org/10.1152/ajprenal.00108.2019>
- Cosio, F. G., Grande, J. P., Larson, T. S., Gloor, J. M., Velosa, J. A., Textor, S. C., Griffin, M. D., & Stegall, M. D. (2005). Kidney allograft fibrosis and atrophy early after living donor transplantation. *American Journal of Transplantation*, 5(5), 1130–1136. <https://doi.org/10.1111/j.1600-6143.2005.00811.x>
- Curtis, M. J., Alexander, S. P. H., Cirino, G., George, C. H., Kendall, D. A., Insel, P. A., Izzo, A. A., Ji, Y., Panettieri, R. A., Patel, H. H., Sobey, C. G., Stanford, S. C., Stanley, P., Stefanska, B., Stephens, G. J., Teixeira, M. M., Vergnolle, N., & Ahluwalia, A. (2022). Planning experiments: Updated guidance on experimental design and analysis and their reporting III. *British Journal of Pharmacology*, 179(15), 3907–3913. <https://doi.org/10.1111/BPH.15868>
- Dinis, P., Nunes, P., Marconi, L., Furriel, F., Parada, B., Moreira, P., Figueiredo, A., Bastos, C., Roseiro, A., Dias, V., Rolo, F., Macário, F., & Mota, A. (2014). Kidney retransplantation: Removal or persistence of the previous failed allograft? *Transplantation Proceedings*, 46(6), 1730–1734. <https://doi.org/10.1016/j.transproceed.2014.05.029>
- Du, C. (2011). Transforming growth factor-beta in kidney transplantation: A double-edged sword. In *Kidney transplantation—New perspectives*. IntechOpen. <https://doi.org/10.5772/20450>
- Findlay, J., Levvy, G. A., & March, C. A. (1958). Inhibition of glycosidases by aldolactones of corresponding configuration. 2. Inhibitors of β -N-

- acetylglucosaminidase. *The Biochemical Journal*, 69, 467–476. <https://doi.org/10.1042/BJO690467>
- Frangogiannis, N. G. (2016). Fibroblast–Extracellular matrix interactions in tissue fibrosis. *Current Pathobiology Reports*, 4(1), 11–18. <https://doi.org/10.1007/S40139-016-0099-1>
- Hira, S. K., Rej, A., Paladhi, A., Singh, R., Saha, J., Mondal, I., Bhattacharyya, S., & Manna, P. P. (2020). Galunisertib drives Treg fragility and promotes dendritic cell-mediated immunity against experimental lymphoma. *iScience*, 23(10), 101623. <https://doi.org/10.1016/J.ISCI.2020.101623>
- Hoeksma, D., Rebolledo, R. A., Hottenrott, M., Bodar, Y. S., Wiersema-Buist, J. J., van Goor, H., & Leuvenink, H. G. (2017). Inadequate antioxidative responses in kidneys of brain-dead rats. *Transplantation*, 101, 746–753. <https://doi.org/10.1097/TP.0000000000001417>
- Holmgard, R. B., Schaer, D. A., Li, Y., Castaneda, S. P., Murphy, M. Y., Xu, X., Inigo, I., Dobkin, J., Manro, J. R., Iversen, P. W., Surguladze, D., Hall, G. E., Novosiadly, R. D., Benhadji, K. A., Plowman, G. D., Kalos, M., & Driscoll, K. E. (2018). Targeting the TGF β pathway with galunisertib, a TGF β RI small molecule inhibitor, promotes anti-tumor immunity leading to durable, complete responses, as monotherapy and in combination with checkpoint blockade. *Journal for Immunotherapy of Cancer*, 6(1), 47. <https://doi.org/10.1186/S40425-018-0356-4>
- Hosgood, S. A., Thompson, E., Moore, T., Wilson, C. H., & Nicholson, M. L. (2018). Normothermic machine perfusion for the assessment and transplantation of declined human kidneys from donation after circulatory death donors. *The British Journal of Surgery*, 105(4), 388–394. <https://doi.org/10.1002/bjs.10733>
- Huang, C. Y., Chung, C. L., Hu, T. H., Chen, J. J., Liu, P. F., & Chen, C. L. (2021). Recent progress in TGF- β inhibitors for cancer therapy. *Bio-medicine & Pharmacotherapy*, 134, 111046. <https://doi.org/10.1016/J.BIOPHA.2020.111046>
- Isaka, Y. (2018). Targeting TGF- β signaling in kidney fibrosis. *International Journal of Molecular Sciences*, 19(9), 2532. <https://doi.org/10.3390/ijms19092532>
- Jensen, M. S., Mutsaers, H. A. M., Tingskov, S. J., Christensen, M., Madsen, M. G., Olinga, P., Kwon, T. H., & Nørregaard, R. (2019). Activation of the prostaglandin E2 EP2 receptor attenuates renal fibrosis in unilateral ureteral obstructed mice and human kidney slices. *Acta Physiologica*, 227(1), 13291. <https://doi.org/10.1111/apha.13291>
- Jochmans, I., Moers, C., Smits, J. M., Leuvenink, H. G. D., Treckmann, J., Paul, A., Rahmel, A., Squifflet, J. P., van Heurn, E., Monbaliu, D., Ploeg, R. J., & Pirenne, J. (2010). Machine perfusion versus cold storage for the preservation of kidneys donated after cardiac death. *Annals of Surgery*, 252(5), 756–764. <https://doi.org/10.1097/SLA.0b013e3181ffc256>
- Kezic, A., Spasojevic, I., Lezica, V., & Bajcetic, M. (2016). Mitochondria-targeted antioxidants: Future perspectives in kidney ischemia reperfusion injury. *Oxidative Medicine and Cellular Longevity*, 2016, 2950503. <https://doi.org/10.1155/2016/2950503>
- Lassen, N. A., Lassen, U., Munck, O., & Thaysen, J. H. (1961). Oxygen consumption and sodium reabsorption by the kidney. Discussion of a theory. *Presse Médicale*, 69, 1259–1260.
- LeBleu, V., Taduri, G., O'Connell, J., Teng, Y., Cooke, V. G., Woda, C., Sugimoto, H., & Kalluri, R. (2013). Origin and function of myofibroblasts in kidney fibrosis. *Nature Medicine*, 19(8), 1047–1053. <https://doi.org/10.1038/NM.3218>
- Li, Y., Zhao, J., Yin, Y., Li, K., Zhang, C., & Zheng, Y. (2022). The role of IL-6 in fibrotic diseases: Molecular and cellular mechanisms. *International Journal of Biological Sciences*, 18(14), 5405–5414. <https://doi.org/10.7150/IJBS.75876>
- Lilley, E., Stanford, S. C., Kendall, D. E., Alexander, S. P., Cirino, G., Docherty, J. R., George, C. H., Insel, P. A., Izzo, A. A., Ji, Y., Panettieri, R. A., Sobey, C. G., Stefanska, B., Stephens, G., Teixeira, M., & Ahluwalia, A. (2020). ARRIVE 2.0 and the *British Journal of Pharmacology*: Updated guidance for 2020. *British Journal of Pharmacology*, 177(16), 3611–3616. <https://doi.org/10.1111/bph.15178>
- Liu, X., Yu, M., Chen, Y., & Zhang, J. (2016). Galunisertib (LY2157299), a transforming growth factor- β receptor I kinase inhibitor, attenuates acute pancreatitis in rats. *Brazilian Journal of Medical and Biological Research*, 49(9), e5388. <https://doi.org/10.1590/1414-431X20165388>
- Luangmonkong, T., Suriguga, S., Bigaeva, E., Boersema, M., Oosterhuis, D., de Jong, K. P., Schuppan, D., Mutsaers, H. A. M., & Olinga, P. (2017). Evaluating the antifibrotic potency of galunisertib in a human ex vivo model of liver fibrosis. *British Journal of Pharmacology*, 174(18), 3107–3117. <https://doi.org/10.1111/bph.13945>
- Matas, A. J., Gillingham, K. J., Humar, A., Kandaswamy, R., Sutherland, D. E. R., Payne, W. D., Dunn, T. B., & Najarian, J. S. (2008). 2202 kidney transplant recipients with 10 years of graft function: What happens next? *American Journal of Transplantation*, 8(11), 2410–2419. <https://doi.org/10.1111/j.1600-6143.2008.02414.x>
- Miller, C. L., & Madsen, J. C. (2021). IL-6 directed therapy in transplantation. *Current Transplantation Reports*, 8(3), 1–204. <https://doi.org/10.1007/S40472-021-00331-4>
- Moers, C., Smits, J. M., Maathuis, M.-H. J., Treckmann, J., van Gelder, F., Napieralski, B. P., van Kasterop-Kutz, M., van der Heide, J. J. H., Squifflet, J. P., van Heurn, E., Kirste, G. R., Rahmel, A., Leuvenink, H. G. D., Paul, A., Pirenne, J., & Ploeg, R. J. (2009). Machine perfusion or cold storage in deceased-donor kidney transplantation. *The New England Journal of Medicine*, 360(1), 7–19. <https://doi.org/10.1056/NEJMc1111038>
- Percie du Serre, N., Hurst, V., Ahluwalia, A., Alam, S., Avey, M. T., Baker, M., Browne, W. J., Clark, A., Cuthill, I. C., Dirnagl, U., Emerson, M., Garner, P., Holgate, S. T., Howells, D. W., Karp, N. A., Lazic, S. E., Lidster, K., MacCallum, C. J., Macleod, M., ... Würbel, H. (2020). The ARRIVE guidelines 2.0: Updated guidelines for reporting animal research. *PLoS Biology*, 18(7), e3000410. <https://doi.org/10.1371/journal.pbio.3000410>
- Porrett, P. M., Orandi, B. J., Kumar, V., Hou, J., Anderson, D., Cozette Killian, A., Hauptfeld-Dolejs, V., Martin, D. E., Macedon, S., Budd, N., Stegner, K. L., Dandro, A., Kokkinaki, M., Kuravi, K. V., Reed, R. D., Fatima, H., Killian, J. T. Jr., Baker, G., Perry, J., ... Locke, J. E. (2022). First clinical-grade porcine kidney xenotransplant using a human decedent model. *American Journal of Transplantation*, 00, 1–17. <https://doi.org/10.1111/AJT.16930>
- Razzaque, M. S., Le, V. T., & Taguchi, T. (2005). Heat shock protein 47 and renal fibrogenesis. *Cellular Stress Responses in Renal Diseases*, 148, 57–69. <https://doi.org/10.1159/000086043>
- Rodón, J., Carducci, M., Sepulveda-Sánchez, J. M., Azaro, A., Calvo, E., Seoane, J., Braña, I., Sicart, E., Gueorguieva, I., Cleverly, A., Pillay, N. S., Desai, D., Estrem, S. T., Paz-Ares, L., Holdhoff, M., Blakeley, J., Lahn, M. M., & Baselga, J. (2015). Pharmacokinetic, pharmacodynamic and biomarker evaluation of transforming growth factor- β receptor I kinase inhibitor, galunisertib, in phase 1 study in patients with advanced cancer. *Investigational New Drugs*, 33(2), 357–370. <https://doi.org/10.1007/S10637-014-0192-4>
- Saritas, T., & Kramann, R. (2021). Kidney allograft fibrosis: Diagnostic and therapeutic strategies. *Transplantation*, 105(10), E114–E130. <https://doi.org/10.1097/TP.0000000000003678>
- Singh, P., Ricksten, S. E., Bragadottir, G., Redfors, B., & Nordquist, L. (2013). Renal oxygenation and haemodynamics in acute kidney injury and chronic kidney disease. *Clinical and Experimental Pharmacology & Physiology*, 40(3), 138–147. <https://doi.org/10.1111/1440-1681.12036>
- Street, J. M., Souza, A. C. P., Alvarez-Prats, A., Horino, T., Hu, X., Yuen, P. S. T., & Star, R. A. (2014). Automated quantification of renal fibrosis with Sirius Red and polarization contrast microscopy. *Physiological Reports*, 2(7), e12088. <https://doi.org/10.14814/PHY2.12088>
- Stribos, E. G. D., Hillebrands, J.-L., Olinga, P., & Mutsaers, H. A. M. (2016). Renal fibrosis in precision-cut kidney slices. *European Journal of Pharmacology*, 790, 57–61. <https://doi.org/10.1016/j.ejphar.2016.06.057>

- Tan, X., Zhang, L., Jiang, Y., Yang, Y., Zhang, W., Li, Y., & Zhang, X. (2013). Postconditioning ameliorates mitochondrial DNA damage and deletion after renal ischemic injury. *Nephrology, Dialysis, Transplantation*, 28(11), 2754–2765. <https://doi.org/10.1093/ndt/gft278>
- Tingskov, S. J., Jensen, M. S., Pedersen, C. E. T., de Araujo, I. B. B. A., Mutsaers, H. A. M., & Nørregaard, R. (2021). Tamoxifen attenuates renal fibrosis in human kidney slices and rats subjected to unilateral ureteral obstruction. *Biomedicine & Pharmacotherapy*, 133, 111003. <https://doi.org/10.1016/j.biopha.2020.111003>
- van Furth, L. A., Leuvenink, H. G., Seras, L., de Graaf, I. A., Olinga, P., & van Leeuwen, L. L. (2022). Exploring porcine precision-cut kidney slices as a model for transplant-related ischemia-reperfusion injury. *Transplantation*, 3(2), 139–151. <https://doi.org/10.3390/TRANSPLANTOLOGY3020015>
- van Leeuwen, L. L., Leuvenink, H. G. D., Olinga, P., & Ruigrok, M. J. R. (2022). Shifting paradigms for suppressing fibrosis in kidney transplants: Supplementing perfusion solutions with anti-fibrotic drugs. *Frontiers in Medicine*, 0(January), 2917. <https://doi.org/10.3389/FMED.2021.806774>
- van Leeuwen, L. L., Ruigrok, M. J. R., Leuvenink, H. G. D., & Olinga, P. (2023). Slice of life: Porcine kidney slices for testing antifibrotic drugs in a transplant setting. *Transplantation*, 4(2), 59–70. <https://doi.org/10.3390/TRANSPLANTOLOGY4020007>
- Vanhove, T., Goldschmeding, R., & Kuypers, D. (2017). Kidney fibrosis. *Transplantation*, 101(4), 713–726. <https://doi.org/10.1097/TP.0000000000001608>
- Vaughan, R. H., Kresse, J. C., Farmer, L. K., Thézéas, M. L., Kessler, B. M., Lindeman, J. H. N., Sharples, E. J., Welsh, G. I., Nørregaard, R., Ploeg, R. J., & Kaisar, M. (2022). Cytoskeletal protein degradation in brain death donor kidneys associates with adverse posttransplant outcomes. *American Journal of Transplantation*, 00, 1–15. <https://doi.org/10.1111/AJT.16912>
- Venema, L. H., Brat, A., Moers, C., 't Hart, N. A., Ploeg, R. J., Hannaert, P., Minor, T., Leuvenink, A. H. G. D., & COPE consortium. (2019). Effects of oxygen during long-term hypothermic machine perfusion in a porcine model of kidney donation after circulatory death. *Transplantation*, 103(10), 2057–2064. <https://doi.org/10.1097/TP.0000000000002728>
- Venema, L. H., van Leeuwen, L. L., Posma, R. A., van Goor, H., Ploeg, R. J., Hannaert, P., Hauet, T., Minor, T., Leuvenink, H. G. D., & on behalf of the COPE Consortium. (2021). Impact of red blood cells on function and metabolism of porcine deceased donor kidneys during normothermic machine perfusion. *Transplantation*, 106, 1170–1179. <https://doi.org/10.1097/TP.0000000000003940>
- Verheijen, M., Lienhard, M., Schrooders, Y., Clayton, O., Nudischer, R., Boerno, S., Timmermann, B., Selevsek, N., Schlapbach, R., Gmuender, H., Gotta, S., Geraedts, J., Herwig, R., Kleinjans, J., & Caiment, F. (2019). DMSO induces drastic changes in human cellular processes and epigenetic landscape in vitro. *Scientific Reports*, 9, 1–12. <https://doi.org/10.1038/s41598-019-40660-0>
- Wang, S., Liang, Y., & Dai, C. (2022). Metabolic regulation of fibroblast activation and proliferation during organ fibrosis. *Kidney Disease*, 8(2), 115–125. <https://doi.org/10.1159/000522417>
- Weissenbacher, A., Lo Faro, L., Boubriak, O., Soares, M. F., Roberts, I. S., Hunter, J. P., Voyce, D., Mikov, N., Cook, A., Ploeg, R. J., Coussios, C. C., & Friend, P. J. (2019). Twenty-four-hour normothermic perfusion of discarded human kidneys with urine recirculation. *American Journal of Transplantation*, 19(1), 178–192. <https://doi.org/10.1111/AJT.14932>
- Yingling, J. M., McMillen, W. T., & Yan, L. (2018). Preclinical assessment of galunisertib (LY2157299 monohydrate), a first-in-class transforming growth factor- β receptor type I inhibitor. *Oncotarget*, 9(6), 6659–6677. <https://doi.org/10.18632/ONCOTARGET.23795>

SUPPORTING INFORMATION

Additional supporting information can be found online in the Supporting Information section at the end of this article.

How to cite this article: van Leeuwen, L. L., Ruigrok, M. J. R., Kessler, B. M., Leuvenink, H. G. D., & Olinga, P. (2024). Targeted delivery of galunisertib using machine perfusion reduces fibrogenesis in an integrated ex vivo renal transplant and fibrogenesis model. *British Journal of Pharmacology*, 181(3), 464–479. <https://doi.org/10.1111/bph.16220>